NJC

Accepted Manuscript

This is an *Accepted Manuscript*, which has been through the Royal Society of Chemistry peer review process and has been accepted for publication.

Accepted Manuscripts are published online shortly after acceptance, before technical editing, formatting and proof reading. Using this free service, authors can make their results available to the community, in citable form, before we publish the edited article. We will replace this *Accepted Manuscript* with the edited and formatted *Advance Article* as soon as it is available.

You can find more information about *Accepted Manuscripts* in the Information for Authors.

Please note that technical editing may introduce minor changes to the text and/or graphics, which may alter content. The journal's standard Terms & Conditions and the Ethical guidelines still apply. In no event shall the Royal Society of Chemistry be held responsible for any errors or omissions in this *Accepted Manuscript* or any consequences arising from the use of any information it contains.

ROYAL SOCIETY OF CHEMISTRY

www.rsc.org/njc

Chemically Exfoliated Nanosilicate Platelets Hybridized Polymer Electrolytes for Solid State Dye Sensitized Solar Cells

Karuppanan Prabakaran, Smita Mohanty* and Sanjay Kumar Nayak

Laboratory for Advanced Research in Polymeric Materials (LARPM),

Central Institute of Plastics Engineering & Technology (CIPET),

Bhubaneswar, Odisha, India-751 024.

*** Dr. Smita Mohanty**

Laboratory for Advanced Research in Polymeric Materials (LARPM)

Central Institute of Plastics Engineering and Technology,

Bhubaneswar-751 024

Odisha, India.

Email: papers.journal@gmail.com

Phone No: 0674 2742852

Fax No: 0674 2740463

Abstract

In this work, a hybrid polymer electrolyte membrane based on poly(ethylene oxide) (PEO)/poly(vinylidene fluoride-co-hexaflouropropylene) (PVDF-HFP) blend containing chemically exfoliated nanosilicate platelets was prepared to replace the conventionally used liquid electrolyte for dye sensitized solar cells (DSSC). The layered montmorillonite nanosilicates were chemically exfoliated using aminopropyltrimethoxy silane (APS). The modifications on nanosilicate by APS molecules were characterized by Fourier infrared spectroscopy (FTIR) and wide angle X-ray diffraction (WAXD). The polymer composite membranes were subjected to FTIR, WAXD and Differential scanning calorimetry (DSC) studies in order to understand the intercalation/exfoliation and crystallinity. The surface and porous structure of composite membranes were examined by scanning electron microscope (SEM) analysis and mercury porosimetry. The porosity and weight uptake enhanced with the addition of surface modified nanoplatelets. The UV-VIS spectra indicated an increase in free ion concentration with the addition of exfoliated nanoplatelets, which led to an increase in the ionic conductivity up to 2.52×10^{-3} S/cm for 6 wt% and it decreased afterwards. On the other hand, same amount of unmodified counterpart achieved an ionic conductivity of about 5.41×10^{-4} S/cm. In addition to this, an increase in ion concentration and ionic diffusion coefficient was found with the addition of surface modified MMT platelets. The linear steady state voltammetry indicated that incorporation of surface modified nanoplatelets reduces the ionic diffusion length and increases the diffusion coefficient to about 4.8×10^{-9}cm^2/s. The photovoltaic performance exhibits an enhanced open circuit voltage (V_{oc}) 0.73 V and short circuit current (J_{sc}) 7.7 mA/cm^2 under the illuminations of 100mW/cm^2.

1. Introduction

In 1991, the first original Dye Sensitized Solar Cell (DSSC) was proposed by O'rigan and Gratzel.[1] After the invention of DSSC, it has attracted significant attention owing to its simple structure, low material cost, and low energy consumption for production.[2] The typical DSSC consists of dye adsorbed TiO_2 as photo anode, I^-/I_3^- redox electrolyte and thin Pt layer as a counter electrode.[3] Till date, the best solar conversion efficiency achieved for a liquid electrolyte based DSSC is about 11-13%.[4] However, low durability, solvent leakage, dye desorption and electrode corrosion in DSSC due to the liquid electrolytes restricts the commercial viability. In order to replace the conventional liquid electrolyte system, many solid state alternatives such as P-type semiconductor, organic hole conductors, room temperature molten salts, polymeric or gel materials comprising redox active electrolyte solution have been studied for DSSC applications.[5-7] Among the solid alternatives, polymer gel electrolytes have several advantages like limited internal shorting, low vapor pressure, excellent contact and filling properties between nano structured photo anode and counter electrode, high ionic conductivity, thermal stability than other solid alternatives.[7] Variety of polymers have been employed as an electrolyte host like PEO, PVDF, PAN, PU, PVDF-HFP, PMMA etc. [9-13] Among them, PVDF-HFP and PEO are selected as the host polymer electrolyte, because PVDF-HFP is photo chemically stable and has high ionic conductivity. Semi-crystalline PVDF gives it the mechanical strength and HFP provides flexibility. [14] Poly (ethylene oxide) (PEO) offers better ion transport by a consolidation of its cation-complexation capability and fast diffusion of chains in the amorphous phase. But the main drawback is its crystallization temperature, which is around 50-60°C. Blending with PVDF-HFP reduces its crystallinity significantly and obtains proper compatibility through the interaction of CF_2 group present in PVDF-HFP and C-O-C in PEO. [15]

Hybridization of inorganic fillers with polymer matrix is a well established technique. It can give combined properties of organic and inorganic materials, like thermal, mechanical and electrical properties. These properties mainly depend upon the size, shape and crystallinity of fillers as well as the bonding between surface functional group of polymer and nanofillers.[16] Till date, TiO_2, Al_2O_3, SiO_2 etc, have been effectively utilized for polymer nanocomposite electrolyte applications. The maximum solar conversion efficiency reported is about 7.2 % employing TiO_2 as fillers.[17] Montmorillonite (MMT) is a type of clay with a high aspect ratio. Its crystal structure consists of layers made up of two tetrahedrally-coordinated silicon atoms fused to an edge-shared octahedral sheet of either aluminium or magnesium hydroxide. The layer thickness is around 1 nm, and the lateral dimensions of these layers are around 100 nm. Stacking of the layers leads to a regular van der Waals gap between the layers called the interlayer or gallery.

The incorporations of MMT nano platelets into the host matrix notably reduce the crystallinity and increase the conductivity through efficient intercalation of polymers. It is also observed that the incorporated nanoclays effectively minimize the ion pair formations. When the polymer chains were confined and entangled by MMT nano platelets, the absorbed electrolytes can migrate diagonally and enhance the conductivity, ion transfer and interfacial properties. Recently, Lee *et al* discovered a novel method to exfoliate montmorillonite (MMT) prepared by using soap-free emulsion polymerization in the presence of MMT to fabricate the nanocomposite latices. The exfoliated MMT sheets were used in ionic liquid based gel electrolyte for dye sensitized solar cells and a conversion efficiency of about 7.8% was achieved. The addition of MMT platelets into gel/polymer electrolytes significantly reduced the charge transfer resistance of various interfaces in DSSC.[18-22]

There are numerous articles on MMT incorporated polymer nanocomposites for cation exchange membrane and mechanical applications using solution intercalations and melt intercalations techniques, respectively[23-25]. To the best of our knowledge, there are no comprehensive articles on chemically exfoliated MMT incorporated PEO/PVDF-HFP composite electrolytes for DSSC applications.

Apart from electrolytes, photo electrode plays the major role in highly efficient dye sensitized solar cells. Various metal oxide semiconductors such as ZnO, ZrO_2, SiO_2, Al_2O_3 and TiO_2 were employed as photo anode materials. Among them TiO_2 has been extensively used as a photo anode material for dye sensitized solar cell applications, but its fast recombination of electron/hole pairs and poor photo-response hinders the photo conversion efficiency. In order to improve the performance of DSSC with TiO_2, several attempts are being carried out by the research community. Another well known material for this application is ZnO, which has higher electron mobility (>150 $cm^2V^{-1}S^{-1}$) and is easily synthesized with various structures than TiO_2. However, the formation of Zn^{2+}/dye complexation on the ZnO nanoparticles surface cause harms the stability and performance of the device[26-29]. When the small amount of ZnO nanoparticles (< 30%) are blended with TiO_2 or covered by TiO_2, it provides better surface morphology, surface area, and transport along with photo electrochemical properties. The photo conversion efficiency of ZnO/TiO_2 based nanocomposites is several orders higher than that of individual components.[30]

In this work, the aforesaid key issue of DSSCs has been taken into account for the development of a solid state dye sensitized solar cell. In this regard, the MMT layered silicate nano clays were chemically exfoliated / delaminated using simple chemical method with APS coupling agent. Further, the effect of exfoliated nanosilicate platelets (modified MMT) on

structural, thermal, morphological, optical and electrochemical properties of PEO/PVDF-HFP was studied. The performance of ZnO/TiO_2 nano composite as a photo electrode material was also explored. The photovoltaic performances of solid state dye sensitized solar cells were studied.

2. Experimental procedure

2.1. Materials

Poly(vinylidenefluoride-co-hexafluoropropylene) (PVdF-HFP, Kynar flex 2801) was supplied by Arkema (India). Poly(ethylene oxide) (PEO) (Mw 5×10^6), aminopropyltrimethoxy silane (APS), triton X-100, chloroplatinic acid hexahydrate and titanium IV- n-butoxide were purchased from Sigma India. Zinc nitrate hexahydrate ($Zn(NO_3)_2 6H_2O$), sodium hydroxide (NaOH), trisodium citrate dihydrate ($HOC(COONa)(CH_2COONa)_2.2H_2O$), anhydrous lithium iodide (LiI) and iodine (I_2) were purchased from Thermo fisher scientific India. The dye, cis-dithio-cyanate-N,N2-bis-(4-carboxylate-4-tetrabutylammoniumcarboxylate-2,2-bipyridine) (N719) was purchased from Solaronix, Switcherland. Anhydrous dimethyl formamide (DMF), ethanol, acetylacetone, nitric acid, propylene carbonate (PC) and ethylene carbonate (EC) were purchased from Himedia, India. 4-*tert*-Butylpyridine (purity > 96%) and 1-Methyl-3-propylimidazolium Iodide (purity > 95%) were purchased from TCI chemicals, India. The conducting FTO glass plates (R_{sh}<10 ohm/cm^2) were supplied by M/s. Shilpa Enterprises, India. Montmorillonite (Na^+MMT) nanoclay was purchased from M/s Southern Clay products, USA.

2.2. Preparation of exfoliated MMT platelets (silane modified MMT)

The nanoclay was dried at 60°C for 10 h in a vacuum oven prior to use. The chemically exfoliated nanosilicate platelets (MMT) were prepared as mentioned the procedure with slight modification from our earlier report.[31]. For silane modification, 1 g of Na^+MMT was dispersed in 75% ethanol solution (250 ml) and vigorously stirred at room temperature for 5 h. Then 2 ml of (3-aminopropyl) trimethoxysilane (APS) was slowly added into the Na^+MMT nanoplatelets suspension and refluxed at 80°C for 24 h. Then the whole Na^+MMT suspension was filtered and washed with distilled water to obtain the silane modified Na^+MMT. In order to achieve the proper exfoliation the silane modified MMT dispersion was introduced into ultra sound sonication for 3 h. The silane modified MMT was named as e-MMT (exfoliated nanosilicate platelets). The chemical exfoliation reaction mechanism of Na^+MMT is depicted in **Scheme 1**

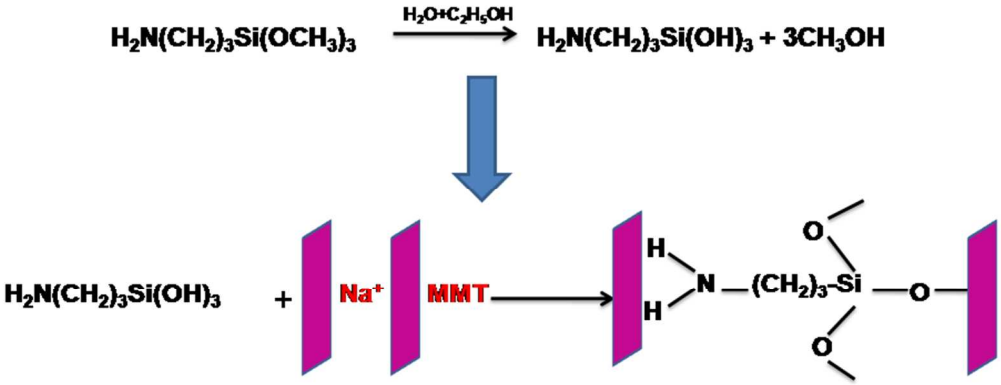

Scheme 1 schematic diagram of Silane modification

2.3. Preparation of polymer blend nanocomposite electrolyte

An optimized composition of (6:4 wt %) of poly (vinylidenefluoride-co-hexafluoropropylene) (PVDF-HFP) and poly(ethylene oxide) (PEO) is dissolved in DMF (99%): glycerol (1%), (solvent and non-solvent, respectively) at 80 °C. Then, predried surface modified (e-MMT) nano platelets were slowly introduced into the polymer solution with different ratios

(1-10 wt %). The mixture was thoroughly mixed under continuous stirring for about 7-8 hours. Subsequently, the mixtures were poured on the glass plate and the solvent was allowed to evaporate at 100°C for 36 h.

2.4. Porosity and electrolyte permeation measurements

The porosity of the membranes was determined by employing gravimetric method. The membranes were soaked in 1- butanol for 2 h and the membrane surface was dried by filter paper afterwards. The membrane weight of the PEO/PVDF-HFP/eMMT membranes was measured before and after absorption immersion.

The porosity was calculated using the following equation (1):

$$\text{Porosity } \varepsilon\ (\%) = 100 \times (W_t - W_o)/\rho V \quad \text{-------} \qquad (1)$$

Where, W_t and W_o is the weight of the wet and dry membrane, respectively. V is the apparent volume of the membrane. ρ is the density of 1-butanol

To determine the electrochemical properties of blend, nanocomposite membranes were soaked in an electrolyte solution containing 0.6M 1-Methyl-3-propylimidazolium Iodide, 0.1 M LiI and 0.05 MI_2 and 0.5 M 4-tert-butylpyridine in EC/PC(1:1 wt%). The weight of the dried and wet composite membranes was measured. After that, the excess liquid electrolyte on the surface of wetted membrane was removed by wiping softly with a tissue paper. The electrolyte uptake was calculated using the following equation (2)

$$\text{Elcetrolyte uptake} = \frac{M_{wet} - M_{dry}}{M_{dry}} X100 \quad ------(2)$$

Where, M_{wet} and M_{dry} are the weight of the membranes after and before soaking in the liquid electrolyte.

2.5. Construction and characterization of solid state dye sensitized solar cells (SSDSSC)

The chemically synthesized ZnO nano sheets and TiO_2 nanoparticles were used as photoanode materials.[29, 30, 32] The dye sensitized photoanode (N 719- ZnO/TiO_2) and counter electrode were prepared as mentioned in our earlier article.[32] The optimized polymer composite electrolyte membrane was sandwiched between N-719 dye adsorbed TiO_2 /ZnO photo anode and Pt coated FTO glass plate with insulating spacer to avoid any short circuit. The schematic diagram of the prepared DSSC is shown in **Scheme 2.**

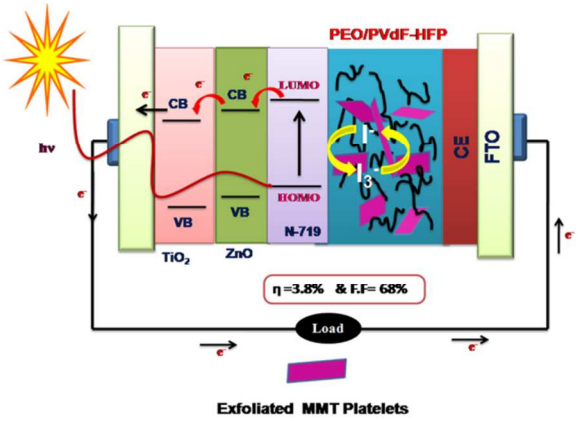

Scheme.2. Solid State sensitized solar cells

2.6. Characterization

FTIR spectra of Nanosilicate (NaMMT and modified MMT) PEO/PVDF-HFP composites were performed on a NICOLET 6700, USA FTIR spectrometer. X-ray analysis of samples was conducted in Schimadzu X-ray diffractometer, Japan using CuK_{α} (1.514Å) at a scanning rate of 5° /min over a 2θ interval from 2° to 80°. SEM characterization of the samples was carried out using a scanning electron microscope (EVO MA 15, M/s Carl Zeiss SMT Ltd, UK). TEM analysis of TiO_2/ZnO nanoparticles was studied by M/S JEOL 1200EX, Japan. Images were taken at an accelerating voltage 100 kV. The mercury porosimetry (Carlo-Erba Porosimeter

2000) was carried out to measure the porosity of the membranes. The mercury diffused under an increasing pressure in the range of 0.01-100 MPa. DSC analysis of the polymer membranes was carried out using DSC, Q20, M/s TA Instruments (USA) equipment. Samples of ≤7 mg was heated from -60°to 200°C, at the heating rate 5°C/min under nitrogen atmosphere. The ionic conductivity measurements were carried out from electrochemical impedance spectroscopy technique by using WonATech-ZiveSP2 (Korea) electrochemical workstation. A perturbation of sinusoidal voltage signal of 10 mV was applied over a frequency range of 1 mHz-1MHz at room temperature. The impedance plots were fitted using Zview2-smart manager software. The samples were sandwiched between circular metal blocking electrodes with a diameter of 10 mm. The thickness of polymer nanocomposite electrolyte membranes was varied from 50 to 300 microns measured by thickness gauge. To characterize the ion (I^-/I_3^-) diffusion, steady state voltammetry was carried by CHI660 electrochemical work station and the scan rate of 5mV/s was applied to obtain the steady state current-voltage curves. The photovoltaic performance of the DSSCs is studied using Oriel Class-A Simulator (M-91900 A, Newport) with Xenon lamp as a light source having intensity of 100mW/cm^2. A computer controlled Auto lab PGSTAT302N electrochemical workstation was used for J-V measurements. The active area of the cell was 0.5 cm^2. To analyze the internal resistance of DSSC, EIS measurements were carried out by Auto lab PGSTAT302N electrochemical workstation with a signal frequency range from 1 mHz-1MHz under the illumination of 100 mWcm^{-2}.

3. Results and discussion

In the following discussion, first the chemical modification of nanosilicate platelets were confirmed and their amount of addition within PEO/PVDF-HFP was optimized at 6 wt% based on ionic conductivity measurements. In order to compare the optimum amount of exfoliated

MMT nanoplatelets (surface modified MMT) with pristine MMT counter parts, the same amount of pristine MMT (6 wt %) was also separately added into the PEO/PVDF-HFP matrix. The optimized compositions such as PEO/PVDF-HFP, PEO/PVDF-HFP-MMT (6 wt% MMT) and PEO/PVDF-HFP-eMMT (6 wt% e-MMT) were further characterized and discussed.

3.1. Conformation of chemical modification nanosilicate platelets by FTIR analysis

Fig.1 shows FTIR spectra of pristine clay (NaMMT) and chemically exfoliated nanosilicate platelets (modified MMT). In the FTIR spectra of the Na-MMT (Fig. 1a), the bands in the range of 3500 and 3700 cm^{-1} and near 3400 cm^{-1} are indicating montmorillonite. The broad peak in the region of 3200-3510 cm^{-1} and 1640 cm^{-1} refers to -OH stretching and bending signifying the existence of entrapped water molecules in the interlayer galleries of NaMMT. The bands around 3620 and 3690 cm^{-1} are due to the presence of –OH stretching of Al–OH and Si–OH of montmorillonite structure.[33]

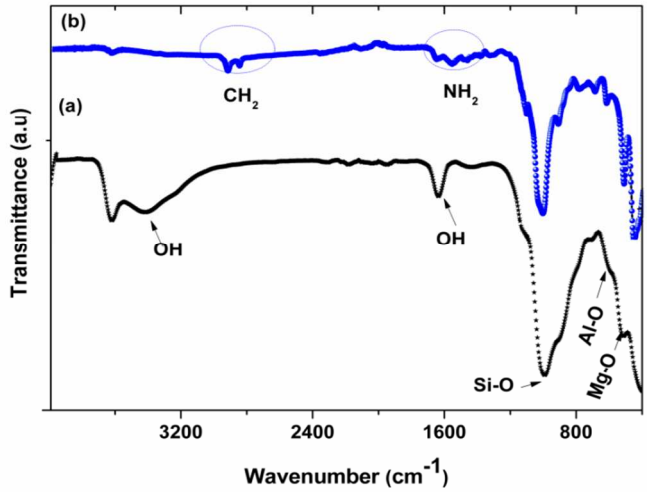

Fig. 1 FTIR spectra of the (a) NaMMT and (b) silane-modified MMT (e-MMT)

The Si–O and Al–O bonds are observed at 1034 and 620 cm^{-1}, respectively and the Mg–O is assigned between 470 and 530 cm^{-1}. [34-35] After treating with APS, new peaks were observed

at 2900-2780 cm^{-1}, which is due to CH or CH_2 structure in the coupling agent. The asymmetric stretching of Si-O-Si (1040 cm^{-1}) was enhanced after the silane modification. Moreover, after APS modification, the intensity of hydroxyl group (-OH) peak at 3520–3200 cm^{-1} and 1640 cm^{-1} was reduced, which indicates that silane moieties are attached on the surface of MMT nano platelets via condensation reaction. The peak observed at 1556 cm^{-1} corresponds to $-NH_2$ bending of functional amino group present in the coupling agent.[35]

3.2. Confirmation of exfoliation of nanosilicate platelets using WAXD

The WAXD analysis is used to examine the intercalation and exfoliation phenomena of layered silicates. The XRD pattern of e-MMT (pristine Na^+MMT, inset Fig. 3) is presented in **Fig. 3.** The WAXD of pristine Na^+MMT exhibits a diffraction peak (d_{001}) at 7.1° with d-space about 13.2Å. After the introduction of silane molecules into Na^+MMT galleries (e-MMT), their diffraction peak shifted to lower angle 2θ = 3.94° (d =20.96 Å). The increased basal spacing of Na-MMT indicates that the introduced aminosilane groups were exfoliated into the silicate layers.[31]

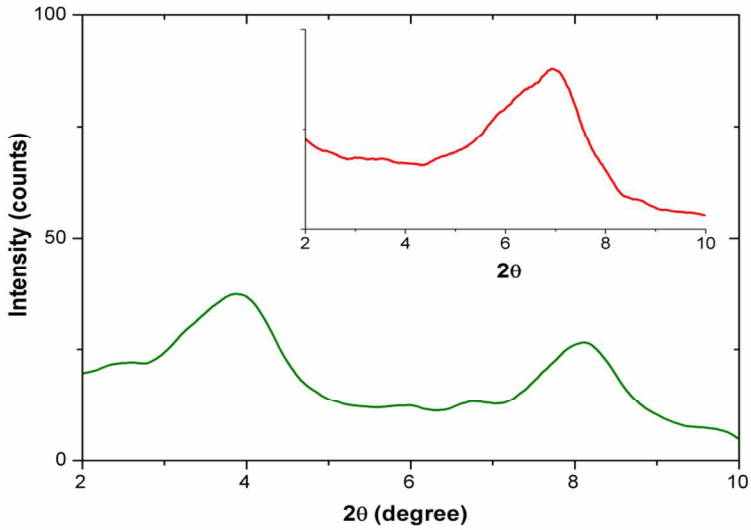

Fig.2. WAXD patterns of exfoliated nanosilicate platelets (e-MMT) (inset Fig pristine Na^+MMT)

3.3. FTIR analysis of polymer nanocomposite membranes

FTIR Transmittance spectra of the PEO/PVdF-HFP and its composite membranes are shown in **Fig. s1**[†]**.** The IR spectra of the electrolyte membranes were characterized in the range of 4000-400 cm^{-1} at room temperature. The main characteristics bands like CF_3 group, CH_2 rocking, CH_2 wagging of vinylidene, C-H bending (out of plane), C-F symmetric stretching, CF_2 stretching, CF_3 symmetrical stretching and CH_2 scissoring vibration of vinylidene group of PVDF-HFP were observed at 759, 853, 870, 971, 1050, 1142, 1280, 1379 and 1407 cm^{-1}, respectively. Similarly, the peaks observed at 1465 and 1354 cm^{-1} is mainly due to the stretching and bending modes of CH_2 in PEO, respectively.[36] The deformed vibration of CH_2 groups appears at 1403 cm^{-1}.[37, 38] The strong absorption band around 1095 cm^{-1} is assigned to the main characteristic peak of non resolved anti-symmetric stretching and symmetric stretching of C-O-C in polymer back bone of pure polycrystalline PEO.[39] The intensity of crystalline characteristics peaks of PEO and PVDF-HFP decreased with the incorporation of pristine MMT nano clay and exfoliated MMT nanoplatelets.

The overall results confirmed that the crystallinity of PEO/PVdF-HFP blend has been completely distorted through the strong interactions with MMT layers and intercalation into the galleries. The effect of nanoplatelets on its structural and thermal properties will be explained in the forthcoming sections. The broad band absorptions of –OH stretching was observed in the range of 3600-3200 cm^{-1}, which is attributed to the large number of intermolecular and intramolecular hydrogen bonds formed by the interactions of solvent and PEO/PVDF-HFP. In

Na-MMT incorporated membrane, the surface hydroxyl group (-OH) within the MMT galleries might be a reason of absorption in these regions. The intensity of –OH stretching was decreased in surface modified MMT incorporated electrolyte membrane, which indicates the hydrolysis condensation reaction of APS molecules present on the MMT nanoplatelets.

3.4. Structural studies of PEO/PVDF-HFP nanocomposites

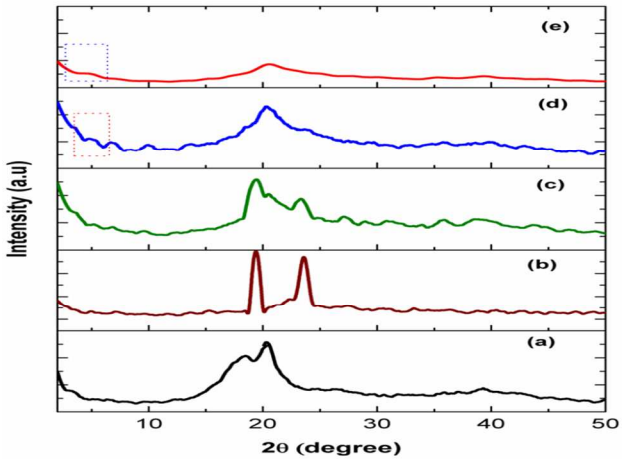

Fig. 3 WAXD pattern of (a) PVDF-HFP, (b) PEO, (c) PEO/PVdF-HFP (d) PEO/PVdF-HFP-MMT and (e) PEO/PVDF-HFP-eMMT nanocomposite

Fig. 3 (a-e) shows the WAXD patterns of PVDF-HFP, PEO, PEO/PVdF-HFP blend and its nanocomposite electrolyte membranes. The characteristics diffraction peaks of PVdF-HFP and PEO were noticed at 18.4°, 20.3°, 26.9° and 19.36° 23.52° for PVdF-HFP and PEO respectively in Fig (3a & 3b).[40, 41] The crystalline peaks of PVdF-HFP were marginally reduced in blend system, which indicates that the PEO is properly blended with PVDF-HFP and the re-crystallization was inhibited. These diffraction peaks were broadened and intensity was decreased with the addition of MMT nano platelets. The decreased intensity may be due to more intercalation of PEO/PVdF-HFP long range chain into the galleries of pristine NaMMT. The absence of diffraction peak in e-MMT incorporated membrane confirms that more reduction in

crystallinity and this behavior might be originated by APS moieties attached in the galleries of nano platelets. The possible intercalation/exfoliations mechanisms are depicted in **Scheme 3.** Additionally, the shifting of characteristic (d_{001}) diffraction peak of pristine MMT (2θ=6.9°) and e-MMT (2θ = 3.94°) to lower angle side (**Fig. 3(d and e**) confirmed that MMT nano platelets are properly dispersed in PEO/PVDF-HFP and might be completely exfoliated.[32] The calculated structural (micro strain and d_{001}) parameters are given in **Table.1.** The increased amorphous nature of polymer matrix might lead to higher ionic conductivity through more amount of electrolyte uptake, which is discussed in next section .[42]

Table 1: Structural parameters of PEO/PVDF-HFP composite electrolytes

Sample	d-space (d_{001}) Å	Micro strain
6% NaMMT	14.54	0.2066
6% e-MMT	22.52	0.2736

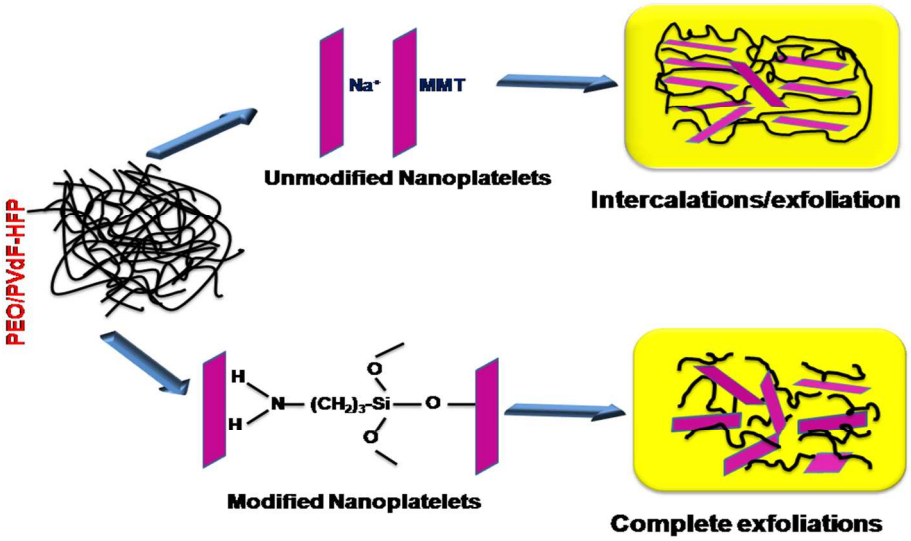

Scheme 3 Intercalation/ exfoliation of nanoplatelets in PEO/PVdF-HFP blends

3.5. Thermal analysis

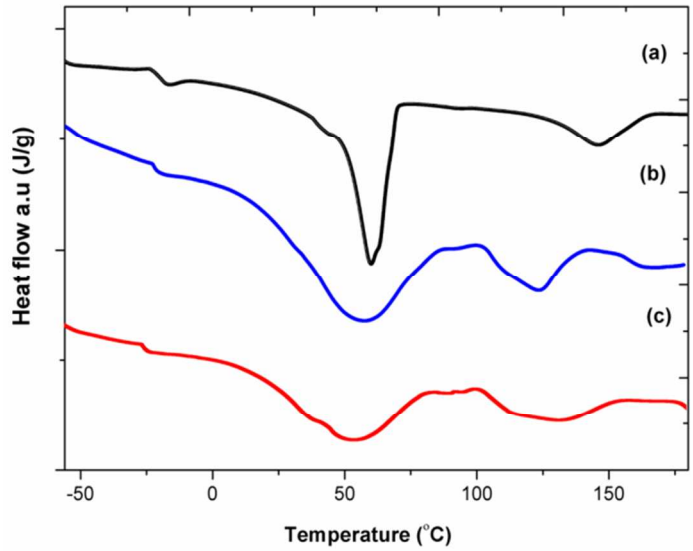

Fig. 4 DSC thermograms of (a) PEO/PVDF-HFP (b) with pristine MMT and (c) e- MMT (Si-MMT) membranes

Fig. 4 shows the DSC thermograms of PEO/PVDF-HFP with pristine NaMMT and chemically exfoliated MMT (silane modified MMT) membranes in range of temperature -60°C to 180°C. As shown in the figure, the melting peaks around -60°C and 150°C of PEO/PVDF-HFP blend are attributed to PEO and PVDF-HFP, respectively. The glass transition temperature of PEO/PVDF-HFP decreased with the addition of MMT nanoclays (**see Table. s1**†), which is attributed to the plasticization effect of nanoplatelets. The addition of nanoplatelets broadened the melting peak of PEO and the melting enthalpy decreased from 45.91 to 35.26 and 33.48 J/g for NaMMT and e-MMT respectively. This suggests that there is reduction in the crystallization of PEO and thereby enhancement in the fraction of free volume. The relative percentage of crystallinity (%χ) of PEO was calculated from the following **equation (3)** and summarized in **Table 2.**

$$\%\chi = \Delta H_m / \Delta H^0_m \times 100\% \qquad \text{---------- (3)}$$

where, ΔH^0_m is the heat of fusion of pure PEO, which is equal to 213.7 Jg^{-1} when, assumed as a 100% crystalline material, [43] ΔH_m is heat of fusion of polymer blend electrolyte.

Similarly, melting enthalpy of PVDF-HFP also decreased from 27.12 to 23.72 J/g. From the **Table.s1**[†]**,** it is observed that reduction in crystallinity for silane modified MMT (chemically exfoliated) is in agreement with XRD results. In e-MMT (silane modified) nanoplatelets incorporated membrane, the MMT nano platelets were completely exfoliated and new silane molecules such as Si-O-Si, NH_2 and CH_2 were anchored on the their surface, which might help to increase the intercalation of polymer chains into the layered structure of nanoclay. The more free volume of composite membranes can help for more electrolyte uptake and easy ions transportation.

3.6. Surface characterization

The surface images of PEO/PVDF-HFP and its composite membranes are shown in **Fig. 5**. It is clearly visible that all membranes have porous structure. It is interesting to note that number of pores are increased with the addition of nano platelets (pristine MMT and exfoliated MMT). **Fig 5.c** shows the sponge-like structure and increased pores size (diameter ~ 3-5 microns) with the incorporation of surface modified nano platelets.

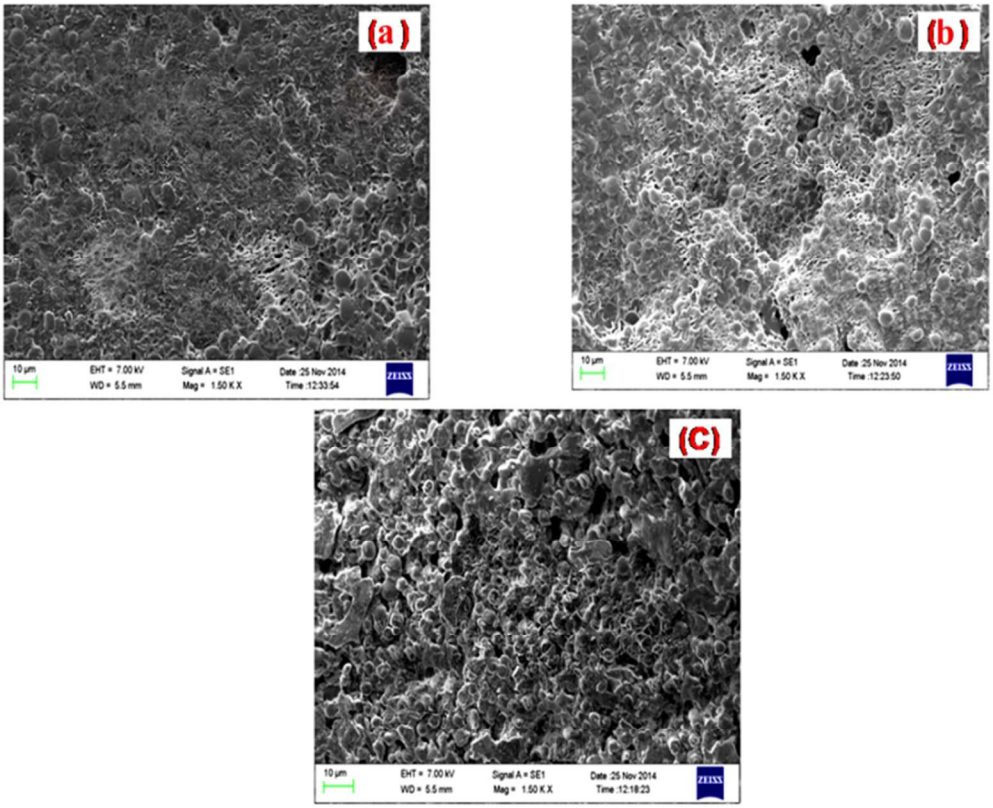

Fig. 5: Surface SEM Images of (a) PEO/PVdF-HFP, (b) PEO/PVdF-HFP/MMT and (c) PEO/PVdF-HFP/eMMT

The porosity and electrolyte uptake measurements of PEO/PVDF-HFP are shown in **Fig. s2**[†]**.** It is seen that porosity of PEO/PVDF-HFP membranes increased with the addition of nano platelets and reaches maximum about 68 % for 6% e-MMT. Beyond this limit there is no significant change in porosity with the further addition of clay. A similar behavior has been observed by R. Prasanth et al, in PVDF-MMT clay composite electrolyte membranes for Li-ion battery applications[44]. Similarly, the amount of liquid electrolyte uptake increased up to 60% for 6 wt% of nanoplatelets and thereafter it decreased. The enhancement in electrolyte uptake with the addition of fillers mainly attributed to the higher affinity of the MMT nanoplatelets toward the solvents of the liquid electrolyte and ionic liquid[45]. The electrolyte uptake is not only related

with the porosity of the membranes, but also to the crystallinity of PEO/PVDF-HFP blend. From the XRD and DSC, it was confirmed that modified MMT (exfoliated MMT) significantly reduced the crystallinity of PEO/PVdF-HFP.

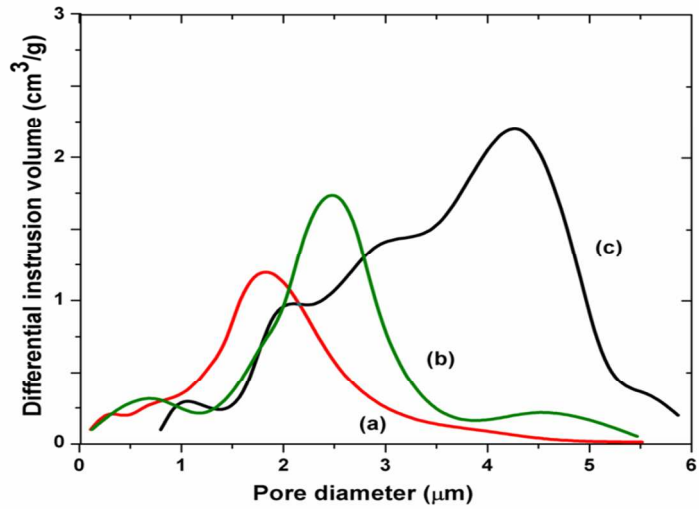

Fig. 6: Pore size distribution curve of (a) PEO/PVDF-HFP, (b) PEO/PVDF-HFP-MMT and (c) PEO/PVDF-HFP-eMMT.

Fig. 6 shows the differential intrusion volume as a function of pore diameter. In Fig.6 (a), it is seen that the pore size of the pure PEO/PVDF-HFP was varying in the range of 0.2 - 4 microns and approximate pore diameter of 1.9 micron. With the addition of pristine MMT nano silicate multiple peaks at 0.6, 2.7 and 4.65 micron were observed and majority of the pores are in the range of 2.7 microns. However in the case of chemically exfoliated nanosilicate plates incorporated PEO/PVDF-HFP membrane, multiple peaks with large pore size in the range of 4-5 microns is seen. The observed results well agreed with the pore size measured from SEM.

The porosity of the membranes was calculated from following relation equation (4)

$$\text{Porosity } (\mathrm{P_M})\% = V_p W \times 100/V \qquad ---------(4)$$

where, V_p is total pore volume (cm^3/g) which deduced from mercury intrusion curve, W is the weight of the samples, V is volume of the samples.[46] The porosity of PEO/PVDF-HFP increased with the addition of pristine MMT and chemically exfoliated nanosilicate platelets (e-MMT). The calculated porosity of PEO/PVDF-HFP composites is higher than porosity measured from porosimetry (P_M). In general, wet type liquid was used in gravimetric method to measure the porosity, hence the calculated porosity showed higher value. The average pore size, pore volume and porosity were measured using mercury porosimetry and is summarized in **Table 2.**

Table 2 Porosimetry data of PEO/PVDF-HFP membranes

Sample	Average Pore size (μm)	Total pore volume (cm^3/g)	Porosity measured from porosimetry (%)	Calculated porosity (P_M) %
PEO/PVDF-HFP	1.5	1.48	30	33
PEO/PVDF-HFP-MMT	2.3	1.96	42	48
PEO/PVDF-HFP-eMMT	4.6	2.9	56	60

3.7. Optical studies

The UV-Vis absorption spectra of MMT and silane treated PEO/PVDF-HFP composite electrolytes membranes are illustrated in **Fig. s3**[†]**.** The peaks of I^- and I_3^- observed about 230 nm and 290 nm for the samples, which is attributed to the absorption of I^- and I_3^- , respectively[40]. The intensity of these two peaks was increased with the incorporation of silane modified nanoplatelets (e-MMT). This indicates that PEO/PVDF-HFP blend absorbed more amount of electrolyte due to their high free volume space. And also the concentration of I^- and I_3^- increased

due to the dissociation of salt by surface hydroxyl group and silane functional group in surface modified MMT nanoplatelets. The porosity and electrolyte uptake of modified MMT incorporated PEO/PVDF-HFP is higher than the PEO/PVDF-HFP/NaMMT membrane. From the above experimental findings it can be concluded that more free anions existed in e-MMT incorporated PEO/PVDF-HFP electrolytes and it is expected to improve the ion transport properties in DSSC.

3.8. Electrochemical characterizations of PEO/PVDF-HFP composite electrolytes

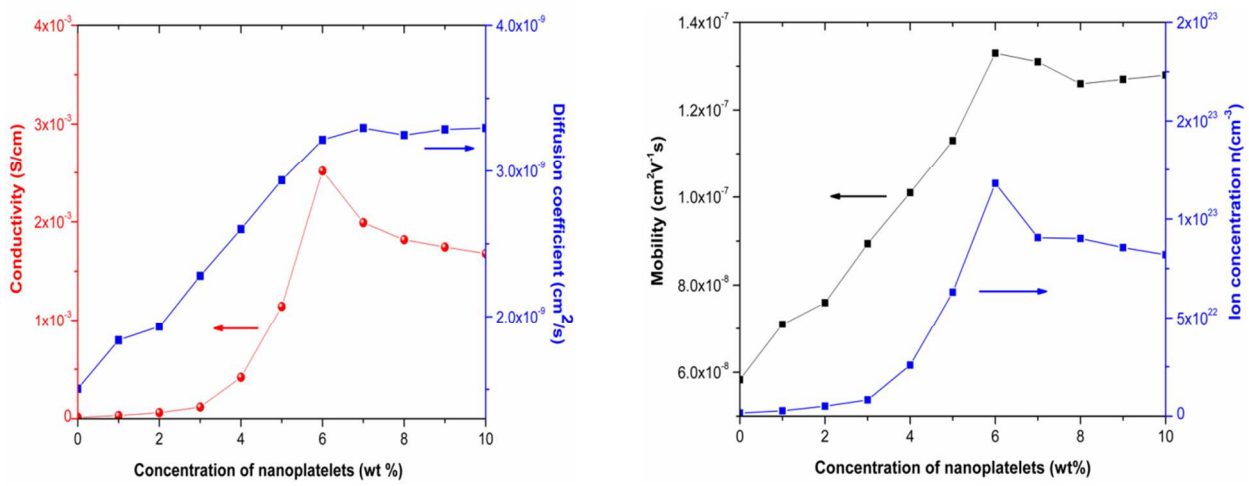

(a) **(b)**

Fig. 7 (a) Ionic conductivity, diffusion Coefficient and (b) Ionic mobility, No. of charge carriers of PEO/PVDF-HFP electrolyte membrane with different amount of modified MMT nanoplatelets

The conductivity, ionic mobility, ionic diffusion co-efficient and ionic concentrations of the PEO/PVDF-HFP gel electrolytes were characterized using EIS technique and shown in **Fig. 7.** The bulk resistance of the electrolytes R_b was calculated from the interception of inclined straight line with the real axis in Nyquist plot (Z' vs Z"). The conductivity (**σ**) of the electrolytes was obtained using the following **Equation (5)**

$$\sigma = {}^{t}/_{R_b A} \qquad \text{--------} (5)$$

Where, t is the thickness of the membrane, R_b is bulk resistance; A is the cross section area of electrode in contact with electrolyte membrane. Other ionic transport parameters such as diffusion coefficient (D), ionic mobility (μ) and charge carrier density were calculated by using the following equations (6, 7 and 8) with the help of fitting parameters and plotted as a function of different amount of nanoplatelets. [47, 48]

$$D = \frac{d^2}{\tau_2 \delta^2} \qquad \text{---------} (6)$$

$$n = \frac{\sigma_{dc}}{e\mu} \qquad \text{---------} (7)$$

$$\mu = \frac{eD}{kT} \qquad \text{---------} (8)$$

Where d= thickness of sample/2, δ=d/λ, λ= $\varepsilon_0 \varepsilon A/k^{-1}$ is the electrical double layer thickness, A is the area of electrolyte membrane, ε_0 is vacuum permittivity, ε dielectric constant of polymer blend electrolytes τ_2=1/ω_2, ω_2 is the angular frequency at which the spike interest at the real impedance axis. The changes in ionic conductivity and diffusion coefficient of the PEO/PVdF-HFP blend electrolyte with the additions of exfoliated nanoplatelets/silane modified (e-MMT) were shown in **Fig**. 7**(a)**. The ionic conductivity of membrane is linearly increased with the addition of exfoliated nanoplates (Silane modified MMT) and attained optimal value of 2.52 mS/cm at 6 wt%. This increasing trend of ionic conductivity is due to the incorporated nanoplatelets, which might influence the kinetics of high molecular weight polymer chain which promotes localized amorphous regions and porosity. The more volume of the pores and high amorphous nature of the blend help to uptake more electrolytes. The mobile charge carriers (iodide/tri-iodide) in the electrolyte can easily move into the porous and liquid like amorphous

structures. Hence, the more electrolytes cause an increase the ionic conductivity and diffusion coefficient.

When the incorporation of nanoplatelets exceeds the optimum level (> 6 wt.%), it reduces the ionic conductivity of PEO/PVDF-HFP electrolytes due to the negative effect of MMT nanoplatelets: as more amount of nanoplatelets induces the aggregation of polymer chains; hence the rate of recrystallization has increased.[49] This crystalline phase of polymer electrolytes block the ions movement, hence ionic mobility and diffusion coefficient also decreased beyond the optimum level of nano platelets as shown in **Fig 7 (a&b)**. The number of ions was found to be same with further additions of MMT, which indicates the 6% wt can dissociate/ coordinate the maximum number of Li^+ and gives the maximum ionic conductivity (**Fig. 7(b**). For comparison, ionic conductivity of same amount (6% wt) of untreated MMT nanoplatelets incorporated PEO/PVdF-HFP was found to be about 5.41×10^{-4} S/cm and it is lower than the same amount of silane modified MMT. In addition, the enhancement in ionic transport properties of silane treated MMT is higher than its unmodified counterpart, which hints the possibility of additional interaction between Li^+ in salt and newly attached surface functional groups within PEO/PVdF-HFP blend electrolyte.

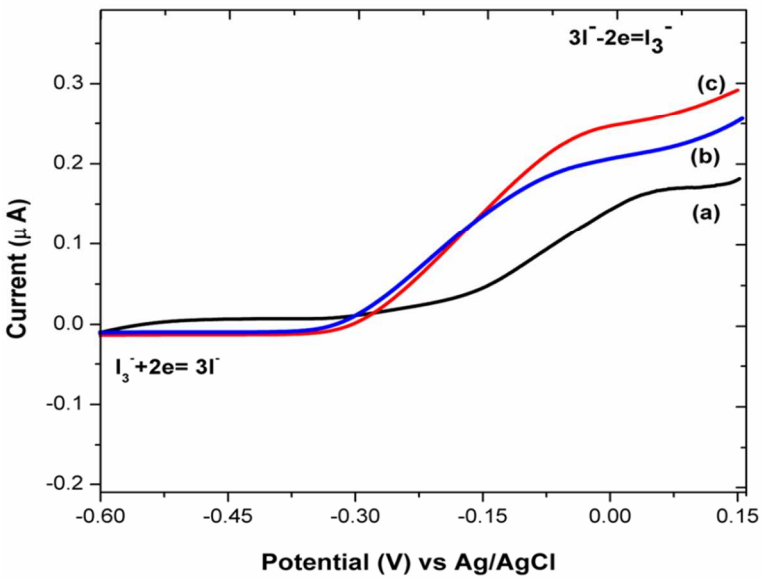

Fig. 8. Steady state voltammograms of (a) PEO/PVdF-HFP (b) PEO/PVdF-HFP /MMT and (c) PEO/PVdF-HFP /eMMT electrolytes

The transport properties of anion (I^-/I_3^-) redox couples in electrolytes are playing a vital role in photovoltaic characteristics of DSSCs. Linear sweep voltammetry technique was used to determine the diffusion coefficient of redox couples (I^-/I_3^-) in the polymer electrolytes. **Fig. 8** shows that steady state voltammograms for PEO/PVDF-HFP composite electrolytes at room temperature. From the cathodic and anodic steady state limiting current (I_{ss}), the apparent diffusion coefficient (D_{app}) of I_3^- and I^-, respectively can be derived from the following equation[50].

$$I_{ss} = 4nRFCD_{app} \quad \text{--------} \ (9)$$

where, n is the number of electrons involved in each electrochemical reaction, F is the Faraday constant, R is the radius of ultra microelectrode, and C is the concentration of electro active species.

The addition of pristine MMT and e-MMT has marginally increased the diffusion coefficient I_3^- and I^- of the PEO/PVdF-HFP blend. This enhancement in diffusion coefficient

indicates that incorporated NaMMT and exfoliated MMT nanoplatelets hinders the long range chain of high molecular weight polymers and facilitates the path way for ionic movements. It is well known that dominant characteristics of I^- diffusion in I^-/I_3^- redox couples within the PEO/PVdF-HFP nanocomposites is mainly due to the smaller ionic radius of I^- compared to I_3^-.[51] These phenomena can be understood that the transport behavior of redox couples I_3^-/I^- in the electrolyte was mainly through the physical diffusion in the liquid like phase called as free volume space in amorphous nature of polymers. The DSC and WAXD results also support the effect of rapid reduction in crystallinity of PEO/PVDF-HFP with the additions of modified MMT nano platelets. The determined ionic diffusion coefficient (I_3^-/I^-) from LSV is also corroborated with EIS results as shown in **Fig. 7** and mentioned in **Table s2**[†]**.** The increased ionic diffusion coefficient (D_{app}) of PEO/PVdF-HFP blends is due to the uniformly distributed modified MMT nanoplatelets. It is understood that the negative charges in the MMT nanoplatelets reduce the attractive force between cation (Li^+) and anion (I^-) present in the electrolyte salt. Hence, apparent diffusion coefficient has been increased.

3.9. Morphological studies of TiO_2/ZnO (SEM and TEM)

The morphology of TiO_2/ZnO composite was examined using SEM and TEM micrographs. **Fig. 9** shows that agglomeration of TiO_2 spherical shaped nanoparticles or grains covered on the flower like structure of nano-ZnO (Fig. 9 (a)). TEM image of TiO_2/ZnO reveals hexagonal shaped thin sheets in the range of 0.5-1 microns (Fig. 9 (b)). These nano/micro sheets combined each other and formed a flower like morphology. The spherical shaped TiO_2 nanoparticles were uniformly distributed on the nano/micro ZnO sheets. The selected area diffraction patterns of TiO_2/ZnO revealed that polycrystalline nature of the nanocomposite.[52]

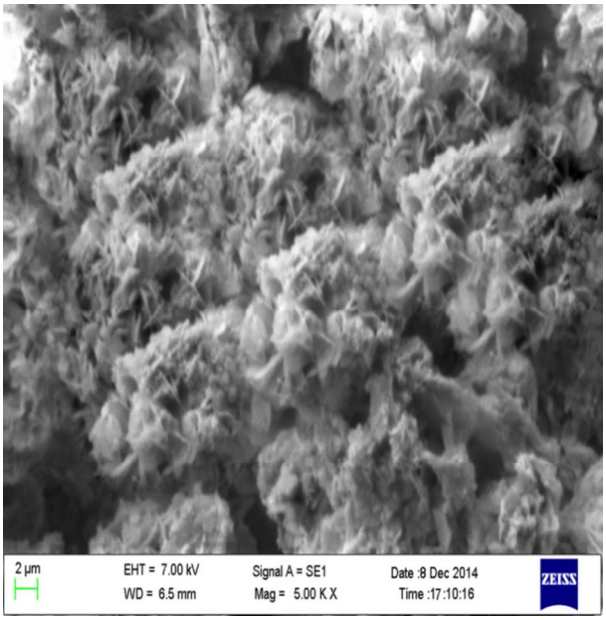

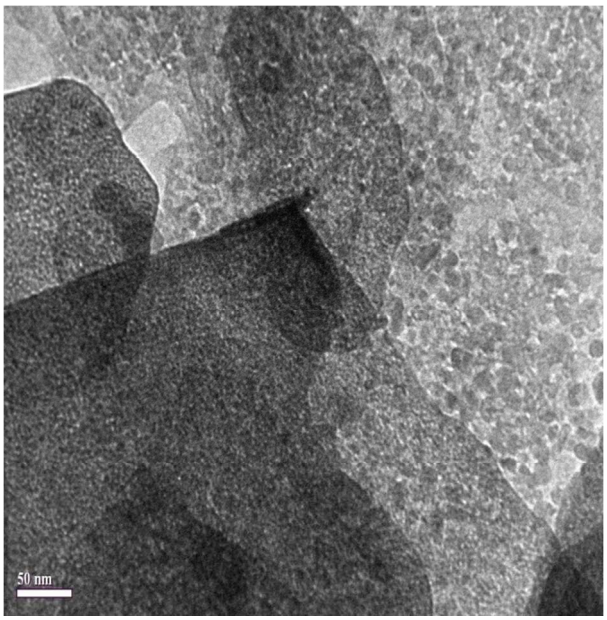

(a) **(b)**

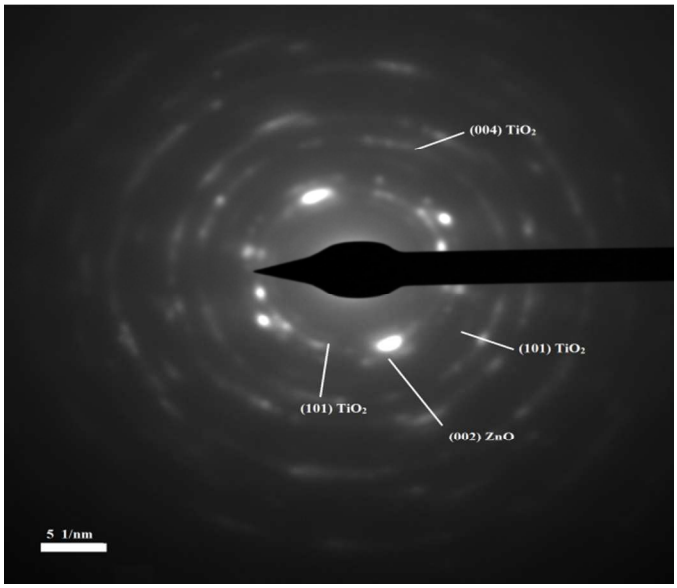

(c)

Fig. 9 (a) SEM (b) TEM images of TiO_2/ZnO and (c) SAED pattern of TiO_2/ZnO

3.10. Photovoltaic performance study

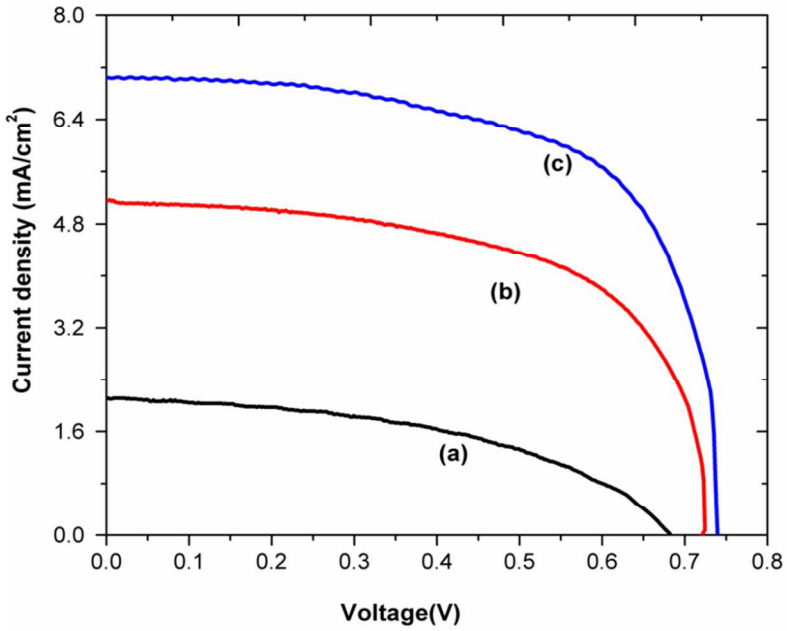

Fig. 10 J-V characteristics curves DSSC based on (a) PEO/PVDF-HFP (b) PEO/PVDF-HFP/MMT and (c) PEO/PVDF-HFP/eMMT

Photocurrent-Voltage (J-V) curves of dye sensitized solar cells (DSSC) were recorded under the light illumination of 100 mW/cm^2 and are depicted in the **Fig. 10.** The measured photovoltaic parameters of all DSSC are summarized in **Table 3.** From the table, it observed that the addition of exfoliated nanoplatelets do not significantly change the open circuit voltage (V_{oc}), but photo-current density (J_{sc}) has been increased from 5.21 mA/cm^2 to 7.7 mA/cm^2 compared with pristine MMT. The enhancement in J_{sc} may be related to the reduction in charge transfer resistance with the additions of exfoliated MMT nanoplatelets. However, the gap between V_{max} and V_{oc} showed a higher difference in all the samples, the values of ΔV/Voc for PEO/PVDF-HFP, PEO/PVDF-HFP/MMT and PEO/PVDF-HFP/e-MMT electrolytes were 33%, 19% and 17%, respectively, which indicated that the serial resistance of DSSC decreased. It is also beneficial for higher fill factor (F.F). Among the electrolytes, chemically exfoliated nano

platelets (silane modified MMT) incorporated electrolyte shows the highest photovoltaic performance. The more amorphous phase of PEO/PVdF-HFP/e-MMT membrane provided easy path for ion migration and this can help rapid regeneration of dye from its oxidized states (D^+), hence performance enhanced. And also the high concentration of I^- and I_3^- ions **(Fig. s3†)** may be the reason to increase the transport properties and favors to achieve the maximum photo-current conversion efficiency (η=3.8%).

Table 3 Photovoltaic parameters for PVDF-HFP and its blend nanocomposite electrolytes

Polymer Electrolytes	V_{oc} V	J_{sc} mA	V_{max} V	I_{max} mA	$\Delta V=V_{oc}-V_{max}$ V	F.F (%)	Efficiency η %
PEO/PVDF-HFP	0.67	2.1	0.45	1.49	0.22	48	0.7
PEO/PVDF-HFP/MMT	0.71	5.2	0.58	3.96	0.13	62	2.3
PEO/PVDF-HFP/eMMT	0.73	7.7	0.61	6.30	0.10	68	3.8

Voc: open circuit voltage (V), Jsc: short circuit current density (mA/cm2), Vmax: maximum voltage (V), Jmax : maximum current density, F.F: fill factor

The solar conversion efficiency (3.8%) of the present device is higher than the efficiency of 3.3% for pure PVDF-PEO based blend nanocomposite electrolytes and 2.82 % of ZnO/TiO_2 photoanode based devices[53, 54]. The comparison of solar conversion efficiency is summarized in Table 4.

Table 4 Comparison on photovoltaic parameters of similar DSSC

Polymer Electrolytes	V_{oc} V	J_{sc} mA	F.F (%)	Efficiency η %	Reference
PEO/PVDF-HFP/e-MMT	0.73	7.7	68	3.8	Present
PEO/PVDF-HFP/modified TiO_2 electrolyte	0.71	6.37	62	2.8	[40]
PEO/PVDF-HFP/SiO_2 electrolyte	0.63	13.3	58	4.9	[55]
ZnO/TiO_2:liquid electrolyte	0.8	6.14	56	2.8	[54]
PEO/PVDF	0.54	2.7	42	0.6	[53]

3.11. Interfacial resistance of DSSC

The charge transfer resistance of various interfaces in DSSC was measured by electrochemical impedance spectroscopy (EIS). The Fig. s4† shows Niquist plots of DSSC based on TiO_2/ZnO nano sheet photo anode and PEO/PVdF-HFP with pristine MMT and e-MMT electrolytes. From, the EIS spectra, it is observed that there are three distinct semi-circles in the measured frequency range of 1 mHz –100 kHz. These semicircles are due to Nernst diffusion within the electrolyte, the electron transfer at the TiO_2-ZnO/electrolyte interface and the redox reaction at the platinum counter electrode. The experimental EIS data fitted with equivalent circuit and charge transfer resistance of each interface has been derived and summarized in **Table s2**†.[56]

R_s is denoted as the series resistance of the electrolytes and electric contacts in the DSSCs. R_{ct1}, R_{ct2} and R_{diff} corresponds to the charge transfer process occurring at the Pt counter

electrode/electrolyte (corresponding to the first arc), the FTO/TiO_2/ZnO/electrolyte interface (corresponding to the second arc) and the Warburg element of the ionic diffusion for the redox-couple (I^-/I_3^-) ion diffusion in the electrolyte (third arc), respectively.[57,58] The DSSC based on silane modified or exfoliated nanoplatelets incorporated PEO/PVDF-HFP electrolyte shows smaller R_{ct2} and R_{diff} than unmodified counterpart. It is mainly due to the more number of pores and increased electrolyte uptake which results in high I^-/I_3^- ion diffusion as well as high ionic conductivity. Effective improvement was achieved in ionic conductivity, mobility, concentration of ions in (**section 3.7)** EIS measurements and high diffusion coefficient of anions (I^-/I_3^-) in LSV studies (**section 3.9**) of PEO/PVDF-HFP/6% e-MMT composites.

4. Conclusion

In summary, poly(ethylene oxide)/polyvinylidene-hexaflouropropylene (PEO/PVDF-HFP) with chemically exfoliated montmorillonite (MMT) nano platelets nanocomposite membranes were successfully prepared for dye sensitized solar cells. The exfoliation of MMT nano clays was achieved using aminopropyltrimethoxy silane and it was confirmed by Fourier infrared spectroscopic analysis and wide angle x-ray diffraction (WAXD). X-ray diffraction and differential scanning calorimetry studies confirmed that the addition of exfoliated nanoplatelets significantly reduced the crystallinity of PEO/PVDF-HFP. The porosity and electrolyte uptake increased with the addition of nanoplatelets. The mercury porosimetry results also suggested that the pore volume and pore diameter has increased for MMT incorporated PEO/PVDF-HFP nanocomposites. The UV-visible spectra indicated that the free ion concentration increased for surface modified MMT. The addition of exfoliated nanoplatelets increase the ionic conductivity up to 2.52×10^{-3} S/cm for 6 wt% and it decreased further, whereas unmodified counterpart

achieved about 5.41×10^{-4} S/cm. Besides that, ionic mobility, ion concentration and ionic diffusion coefficient also found to increase with the incorporation of exfoliated MMT platelets. It was observed from linear steady state voltammetry that the incorporation of surface modified nanoplatelets reduce the ionic diffusion length, thereby enhancing the ionic diffusion coefficient (I^-) upto 4.8×10^{-9} cm^2/s. The solid state dye sensitized solar cell has been fabricated by using optimized composition of polymer nanocomposites electrolyte and TiO_2/ZnO composite as a photo anode. The presence of exfoliated MMT nanoplatelets in the electrolyte significantly improves the photovoltaic performance of DSSC. The optimal solar conversion efficiency of DSSC with exfoliated MMT nanoplatelets/ PEO/PVDF-HFP electrolytes is determined as 3.8%, which is about 65% higher than that of the pristine MMT incorporated electrolyte based DSSC. The results suggest that reinforcement of exfoliated MMT nanoplatelets is an effective approach to enhance the transport properties within polymer electrolytes.

Acknowledgement

One of the authors (K.Prabakaran) is thankful to Prof. P. Ramasamy and Dr. M. Senthil Pandian, SSN Research Centre, Chennai, Tamilnadu for their support of photo anode preparation. Also thankful to Ms. Sriparna De Mr.R.K. Swain and B.Nayak, LARPM, CIPET, Bhubaneswar for their assistance in morphological and thermal characterizations.

REFERENCES

1. B. O. Regan and M. Gratzel, Nature, 1991, **353**, 737.
2. Y.C.Wang, K.C.Huang, R.X.Dong, C.T.Liu, C.C. Wang, K.C.Ho and J.J. Lin, Journal of Materials Chemistry, 2012, **22**, 6982.
3. C. Chen, Y. Li, X. Sun,F. Xie and M. Wei, New J. Chem., 2014, **38**, 4465.
4. S.Mathew, A. Yella, P. Gao, R. H.Baker, B. F. E. Curchod,N. A.Astani, I. Tavernelli, U.Rothlisberger, M. K. Nazeeruddin and M. Grätzel, *Nature Chemistry* 2014, **6**, 242.
5. J. Bandara, J. P. Yasomanee, Semicond. Sci. Technol. 2007, **22**, 20.
6. Y.S.Kwon, J. Lim, I. Song, I.Y. Song, W.S. Shin, S.J. Moon and T. Park, J. Mater. Chem., 2012, **22**, 8641.
7. L.Tao , Z.Huo, S. Dai, Y. Ding , J.Zhu , C. Zhang , B. Zhang , J.Yao, M.K. Nazeeruddin and M. Gratzel , J. Phys. Chem. C, 2014, **118,** 16718.
8. A. L. Sharma and A. K. Thakur, Ionics, 2010, **16,** 339.
9. Y. Duan, Q. Tang, Y.Chen, Z. Zhao, Y. Lv, M. Hou, P. Yang, B. He and L. Yu, Journal of Materials Chemistry A, 2015, **3**, 5368.
10. H.C.Lee, H.Cheol, A. M. Shaheer, P.J. Geun, K.K.Ju, S.K.Lee, S. K. Yang and O.Bong, J Nanosci Nanotechnol. 2010, **10,** 3502.
11. H.W. Ho, W.Y. Cheng, Y.C. Lo, T.C. Wei and S.Y. Lu, ACS Appl. Mater. Interfaces 2014, **6**, 17518.
12. H.S. Lee, C.H. Han, Y.M. Sung, S.S. Sekhon and K.J. Kim, Current Applied Physics 2011, **11**, S158.
13. F. S. Freitas , J.N.D Freitas , B.I. Ito ,.A. De Paoli and A. F. Nogueira, ACS Appl. Mater. Interfaces, 2009, **1 (12)**, 2870.

14. C.M. Costa, M.M. Silva and S. L. Méndez , RSC Adv., 2013,**3**, 11404.

15. C.A. Nguyen, S. Xiong J. Ma, X. Lu and P.S. Lee , *Phys. Chem. Chem. Phys.*, 2011,13, 13319.

16. A.K. Nath and A. Kumar, Journal of Membrane Science, 2014, **453**, 192.

17. M.S. Kanga, K.S. Ahnb and J.W. Lee, J. of power sources, , 2008, **18**, 896.

18. E. Manias , A. Touny , L. Wu , K. Strawhecker , B. Lu , and T. C. Chung, Chem. Mater., 2001, **13,** 3516.

19. Y. Geng, Y. Shi, L. Wang, B. Ma, R. Gao, Y. Zhu, H. Dong and Y. Qiu, Phys. Chem. Chem. Phys., 2011, **13**, 2417.

20. C-H. Lee, T.H. Weng, K. Y. Liu, K. J. Lin and K-F. Lin, Journal of Applied Polymer Science, 2010, **118**, 652.

21. C-H. Lee, K-Y. Liu, S-H. Chang, K-J. Lin, J-J. Lin, K-F. Lin and K-C.Ho Journal of Colloid and Interface Science, 2011, **363**, 635.

22. C-W.Tu, K-Y. Liu, A-T. Chien, M-H. Yen, T. H. Weng, K-C. Ho **and** K-F Lin, J. Polymer Science: Part A: Polymer Chem. 2008, **46**, 47.

23. P. Vickraman, K. Purushothaman, B. Karthikeyan and C. S. Semler, Ionics 2014, **20**, 681.

24. A. K. Nath and A. Kumar Ionics 2013, **19**, 1393.

25. P. J. Jandas, S. Mohanty, and S. K. Nayak, Journal of Polymers, 2013, **2013**, 1.

26. X. Luan and Y. Wang, J. Phys. Chem. C, 2014, **118**, 18917.

27. C. Lin, F.Y.Tsai, M.H. Lee, C.H. Lee, T.C. Tien, L.P. Wang and S.Y. Tsai, J. Mater. Chem., 2009, **19**, 2999.

28. Y. Sun, L. Wang, X. Yu and K. Chen, Cryst. Eng. Comm, 2012, **14**, 3199.

29. V. Manthina, J. Pablo, C. Baena, G. Liu and A.G. Agrios J. Phys. Chem. C, 2012, **116**, 23864.

30. N. Rajkumar, S.S. Kanamani and K.Ramachandran, Science of Advanced Materials, 2011, **4**, 627.

31. K. Prabakaran, S. Mohanty and S.K. Nayak, Int. J.of Plast.Technology, 2014, DOI:10.1007/s12588-014-9089-5

32. K. Prabakaran, S. Mohanty and S.K. Nayak, ceramics international, 2015, DOI:10.1016/j.ceramint.2015.05.151

33. W. S. Chow and S. S. Neoh, Journal of applied polymer science, 2009, **114**, 3967.

34. Y.P Wang, X.H. Gao, R.M. Wang, H.G. Liu, C. Yang and Y.B. Xiong, Reactive & Functional polymers, 2008, **68**, 1170.

35. S.J. Park, B.J.Kim, D.I. Seo, K.Y. Rhee and Y.Y. Lyu, Materials Science and Engineering A, 2009, **526**, 74.

36. M. Deka and A. Kumar, Bull. Mater. Sci.,2009, **32,** 627.

37. S. Rajendran, O. Mahendran and R. Kannan, Mater. Chem. Phys., 2002, **74,** 52.

38. K. Prabakaran, S. Mohanty and S.K. Nayak, J. Solid State Electrochem., 2015, DOI 10.1007/s10008-015-2883-y.

39. Y.Y. Hao, J. Peng, W. Furong, W.Lefu and L. Xuehui, Science China Chemistry, 2012, **55,** 1608.

40. K. Prabakaran, S. Mohanty and S.K. Nayak, RSC Adv., 2015, **5**, 40491.

41. Y. Liu, J.Y. Lee and L. Hong, Solid State Ionics, 2002, **150**, 317.

42. R. Prasanth, N. Shubha, H.H. Hong and M. Srinivasan, Journal of Power Sources, 2014, **245**, 283**.**

43. Y.Yang, C.Zhou, S. Xu, H. Hu, B. Chen, J. Zhang, W. Liu and X.Z. Zhao, S. Wu, Journal of Power Sources. 2008, **185**, 1492.

44. R. Prasanth, N. Shubha, H. H. Hng and M. Srinivasan, European Polymer Journal, 2013, **49**, 307.

45. Y. Ran, Z. Yin, Z. Ding, H. Guo and J. Yang, Ionics, 2013, **19**, 757.

46. I. K. Kwon, S. Kidoaki and T. Matsuda, Biomaterials, 2005, **26**, 3929.

47. A.K.Arof, M. Naeem, F. Hameed, W.J.M.S.R.Jayasundara, M.A.Careem, L.P.Teo and M.H. Buraidah, Optical and quantum electronics, 2014, **46**, 143.

48. W.A.Van Schalkwijk and B. Scrosati (Eds), Advances in Lithium Ion Batteries, Kluwer Academic/Plenum Publishers, New York, 2002.

49. K. Prabakaran, S. Mohanty and S.K. Nayak, J. Mater Sci: Mater. Electron., 2015, 26, 3887.

50. C. Y. Neo, N. K. Gopalan and J. Ouyang, J. Mater. Chem. A, 2014, 2, 9226.

51. A.J. Bard and L.R. Faulkner Electrochemical Methods: Fundamentals and Applications (second ed.) John Wiley & Sons, New York (2001), pp. 171–175.

52. A. Sarkar, A. K. Singh, G. G. Khan, D. Sarkar and K. Mandal, RSC Adv., 2014, **4**, 55629.

53. Y. Yang, J. Zhang, C. Zhou, S. Wu, S. Xu, W. Liu, H. Han, B. Chen and X-Z. Zhao, J. Phys. Chem. B 2008, **112**, 6594.

54. J. Liu, A. Wei, Y. Zhao, K. Lin and F. Luo, J Mater Sci: Mater. Electron., 2014, **25**, 1122.

55. J. Zhang, Y. Yang, S. Wu, S. Xu, C. Zhou, H. Hu, B. Chen, X. Xiong, B. Sebo, H. Han and X. Zhao, Nanotechnology, 2008, **19**, 245202.

56. C.W. Tu, K.Y. Liu, K.C. Ho, A.T. Chien, K.F. Lin, M.H. Yen and T.H. Weng, Journal of Polymer Science: Part A: Polymer Chemistry, 2008, **46**, 47.

57. M. Wang and S. Dong, Journal of Power Sources, 2007, **170**, 425.

58. K. Prabakaran, Akshaya K. Palai, Smita Mohanty and Sanjay Kumar Nayak, RSC, Adv., 2015, 5, 66563.

Graphical Abstract

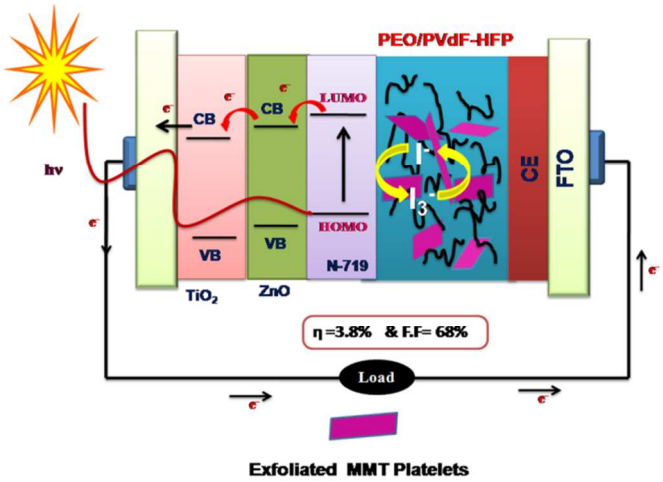

Exfoliated MMT nanoplatelets incorporated PEO/PVdF-HFP electrolyte and TiO_2/ZnO photoanode based DSSC showed improved solar energy conversion efficiency of about 3.8%.